ISIJ International, Vol. 40 (2000), No. 7, pp. 719–724

# Aging Behaviour of 25Cr–17Mn High Nitrogen Duplex Stainless Steel

Izabel Fernanda MACHADO and Angelo Fernando PADILHA[1)]

Institute of Science and Technology (ICET), Paulista University (UNIP), São Paulo, Brazil. E-mail: izabelfm@uol.com.br.
1) Department of Metallurgical and Materials Engineering, University of São Paulo (USP), Av. Prof. Mello Moraes, 2463, 05508-900, São Paulo, Brazil. E-mail: padilha@usp.br.

(*Received on January 24, 1999; accepted in final form on March 22, 2000*)

The precipitation behaviour of a nickel free stainless steel containing 25 % chromium, 17 % manganese and 0.54 % nitrogen, with duplex ferritic–austenitic microstructure, was studied using several complementary techniques of microstructural analysis after aging heat treatments between 600 and 1 000°C for periods of time between 15 and 6 000 min. During aging heat treatments, ferrite was decomposed into sigma phase and austenite by a eutectoid reaction, like in the Fe–Cr–Ni duplex stainless steel. Chromium nitride precipitation occurred in austenite, which had a high nitrogen supersaturation. Some peculiar aspects were observed in this austenite during its phase transformations. Chromium nitride precipitation occurred discontinuously in a lamellar morphology, such as pearlite in carbon steels. This kind of precipitation is not an ordinary observation in duplex stainless steels and the high levels of nitrogen in austenite can induce this type of precipitation, which has not been previously reported in duplex stainless steels. After chromium nitride precipitation in austenite, it was also observed sigma phase formation near the cells or colonies of discontinuously precipitated chromium nitride. Sigma phase formation was made possible by the depletion of nitrogen in those regions. Time–temperature–transformation (precipitation) diagrams were determined.

KEY WORDS: duplex stainless steel; nitride precipitation; sigma phase precipitation; TTT diagrams.

## 1. Introduction

Nitrogen in solid solution in stainless steels improves their mechanical properties and corrosion resistance.[1)] It also causes a great enlargement of the austenitic field.[1–3)] On the other hand, the solubility of nitrogen in Fe–Cr–Ni or Fe–Cr–Mn–Ni austenites decreases considerably with decreasing temperature[1–3)] and chromium nitride precipitation can take place. The aging behaviour of the 18%Cr–18%Mn austenitic stainless steel containing high level of nitrogen (0.6 wt%) has been studied.[4)] The exposure of this steel to temperatures between 700 and 900°C caused $Cr_2N$ precipitation.[4)] Nitride precipitation in high nitrogen austenitic stainless steels can occur both continuously or discontinuously, however discontinuous precipitation is favoured at high nitrogen supersaturation.[2,3)] Nitride precipitation is deleterious to the steel mechanical and corrosion properties. Sigma phase precipitation was not mentioned in the work done by Presser and Silcock.[4)] On the other hand, sigma precipitation is very common and abundant in duplex stainless steels containing lower levels of nitrogen[5)] and it was also detected in high nitrogen austenitic stainless steels after nitride precipitation.[2,3,6)] Sigma phase precipitation shows much faster kinetics in duplex stainless steels than in single-phase austenitic or ferritic types.[5,7)] The ferrite/austenite interfaces act as preferred sites for sigma nucleation and besides that diffusion is much faster in ferrite than in austenite. Sigma phase causes chromium impoverishment near the precipitates and decreases of the corrosion resistance. Furthermore, sigma phase is very hard, fragile and it induces the deterioration of impact toughness.[8)]

In this work a nickel free 25%Cr–17%Mn–0.54%N (in wt%) steel was studied, which has a duplex ferritic–austenitic microstructure. The nitrogen and manganese contents are relatively high, but not enough to completely stabilize the austenite. The main objective of this investigation was to study the precipitation of nitrides and other phases, especially sigma, in a wide range of temperatures and times with the aid of various complementary techniques of microstructural analysis.

## 2. Experimental Procedure

The stainless steel studied in this work, initially had a cast duplex ferritic–austenitic microstructure. The solution annealing heat treatment was done at 1 050°C for 2 h followed by quenching in water. Its chemical composition (wt%) was 25.80% Cr, 17.21% Mn, 0.035% C, 0.54% N, 1.12% Si, 0.11% Ni, 0.04% V, 0.026% Al, 0.012% P and 0.04% S. After solution annealing, aging heat treatments were carried out in the temperature range of 600 to 1 000°C, for periods of time between 15 and 6 000 min. The samples were quenched in water after aging heat treatments. The dimensions of all the heat treated specimens

were about 5×5×5 mm in order to avoid phase transformations during cooling (quenching in water).

The microstructures were analyzed by several complementary techniques. The metallographic sample preparation consisted of grinding with #1000 emery paper, 1 $\mu$m diamond polishing and further electrolytic etching. The electrolyte composition was 700 ml ethanol, 120 ml distilled water, 100 ml 2-butoxyethanol (butyl glycol) and 80 ml perchloric acid (60%). The electrolyte was kept at 0°C and a tension of 20 V was applied for 20 sec. The specimens for general microscopical examinations were etched at 70°C for 20 to 60 sec in V2A-Beize etchant.[9] The microstructures of the samples were examined by optical and scanning electron microscopy. The crystal structures of the various phases were determined by X-ray diffraction measurements on polished surfaces with the aid of a diffractometer. Copper K$\alpha$1 radiation was used. The chemical compositions of the different phases were investigated by energy dispersive analysis. The amount of ferromagnetic phases was determined using the magnetic induction method (Fischer Permascope® M11 D; with a 0.1% ferrite detection limit). Vickers hardness (with a 0.2 kg load) of all the specimens was also measured.

## 3. Results

The results will be presented in the two major sections as follows: solution annealed condition and aged condition. The aged condition will be subdivided in three subsections: phase transformations in ferrite, phase transformations in austenite and time–temperature–transformation (TTT) diagrams.

### 3.1. Solution Annealed Condition

The microstructure and the results of X-ray diffraction of the studied steel in the solution-annealed condition are shown in **Figs. 1** and **2**, respectively. Vickers microhardness, volumetric fraction of the phases and chemical composition of ferrite and austenite, by using scanning electron microscopy with energy dispersive analysis, are shown in **Table 1**.

### 3.2. Aged Condition

Aging heat treatments between 600 and 1 000°C led to several phase transformations in the 25%Cr–17%Mn–0.54%N duplex stainless steel samples. **Figure 3** shows the results of X-ray diffraction of the sample aged at 860°C for 10 h. The diffractometer pattern shows the presence of sigma phase[11] and chromium nitride ($(Cr,Fe)_2N$)[12] in this sample. On the other hand, ferrite was not present after the aging heat treatment.

For the sake of simplicity results of phase transformations in ferrite and in austenite are presented separately in the following sections.

3.2.1. Phase Transformations in Ferrite.

Ferrite is a ferromagnetic phase and some of its phase transformations can be followed by measuring this property. After aging heat treatments, the magnetism of all the samples was measured by using a ferritoscope. These results are displayed in **Table 2**. The aged samples show a decrease of the magnetism as a consequence of ferrite decomposition into another phase or other phases. Ferrite decomposition occurred rapidly in the range of temperatures between 700 and 860°C.

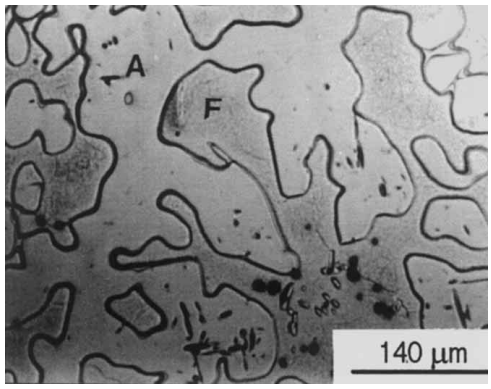


**Fig. 1.** Microstructure of the 25%Cr–17%Mn–0.54%N steel in the solution annealed condition: 1 050°C for 2 h followed by quenching in water. Optical microscopy. Etching: V2A Beize. F indicates ferrite and A indicates austenite.

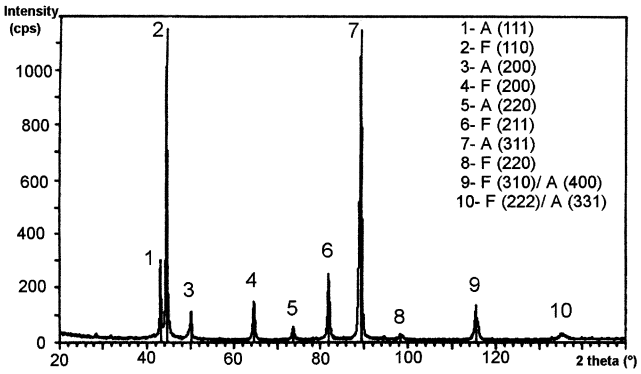


**Fig. 2.** X-ray diffraction pattern of the 25%Cr–17%Mn–0.54%-N steel in the solution annealed condition: 1 050°C for 2 h followed by quenching in water. CuK$\alpha$1 radiation. F indicates ferrite and A indicates austenite.

**Table 1.** Volumetric fraction, Vickers microhardness and chemical composition by using scanning electron microscopy with energy dispersive analysis of the phases of the 25%Cr–17%Mn–0.54%N steel solution annealed at 1 050°C for 2 h and quenched in water.

| Phases | Ferrite | Austenite |
|---|---|---|
| Volumetric fraction of the phases | 0. 47 | 0.53 |
| Vickers microhardness (0.2 Kg) | 274±20 | 290±16 |
| Chemical composition (wt.%) | Fe; 26.8 Cr; 16.4 Mn; 1.2 Si | Fe; 26.6Cr; 18.8Mn; 0.96Si; 1.0 N [10] |

Scanning electron microscope images of some samples after aging heat treatments were taken by using secondary or back scattered electrons, as shown by **Figs. 4** and **5**, respectively. These micrographs show the presence of two phases in the transformed parent ferrite as a result of ferrite decomposition.

In the same temperature range of ferrite decomposition, sigma phase could be identified by using X-ray diffraction (Fig. 3). Austenite was also identified in the same time–temperature range by using scanning electron microscopy with back scattered electrons images and chemical microanalysis. **Table 3** shows the chemical composition results of phase analysis.

**Table 2.** Magnetic measurements (in vol %) of aged samples using a ferritoscope.

| Sample | 15 min | 30 min | 60 min | 120 min | 240 min | 360 min | 600 min | 1440 min | 2880 min | 6000 min |
|---|---|---|---|---|---|---|---|---|---|---|
| 610°C | - | - | - | - | - | - | - | 0.5±0.1 | - | - |
| 700°C | - | 0.6±0.1 | 0.3±0.1 | - | - | - | 0.3±0.1 | - | - | - |
| 730°C | - | - | 0.3±0.1 | - | 0.6±0.1 | 0 | - | 0.1±0.1 | 0 | - |
| 785°C | 0.9±0.2 | - | 0.6±0.3 | - | - | - | - | - | - | - |
| 810°C | 3.0±0.4 | - | 0.6±0.1 | 0.3±0.1 | - | - | - | 0.2±0.2 | - | - |
| 850°C | - | 3.6±1.2 | - | - | 2.8±1.2 | - | - | - | - | 0 |
| 860°C | 13.7±2.5 | - | 1.2±0.2 | - | - | - | 0 | - | - | 0.2±0.2 |
| 900°C | 28.2±3.6 | - | 4.4±0.9 | - | -- | - | - | - | - | - |
| 950°C | - | - | 36.9±1.8 | - | - | - | - | - | - | - |
| 1000°C | 40.4±2.9 | - | - | - | - | - | - | - | - | - |

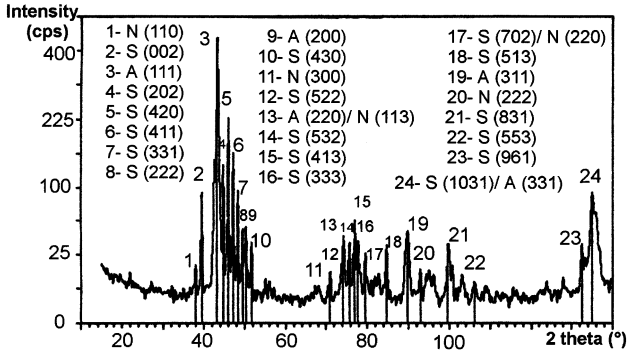


**Fig. 3.** X-ray diffraction pattern of the 25%Cr–17%Mn–0.54%N steel in the aged condition: 860°C for 10 h followed by quenching in water. CuK$\alpha$1 radiation. A indicates austenite, N indicates chromium nitride and S indicates sigma phase.

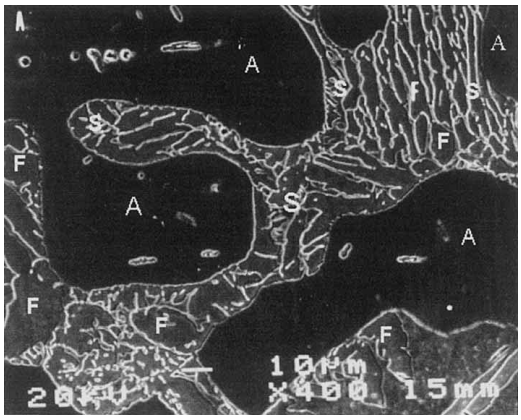


**Fig. 4.** Scanning electron microscopy micrograph of the sample aged at 900°C for 1 h followed by quenching in water. Secondary electrons. A indicates austenite, S indicates sigma phase and F indicates the parent ferrite. Etching: V2A-Beize.

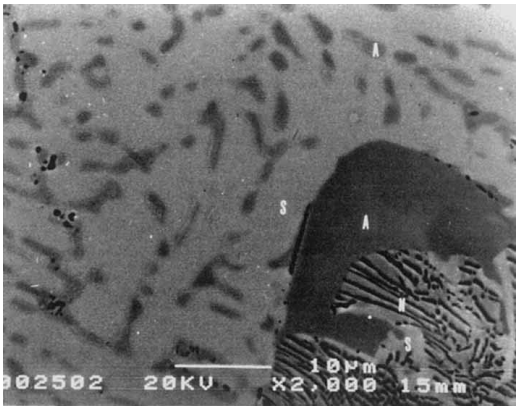


**Fig. 5.** Scanning electron microscopy micrograph of the sample aged at 860°C for 10 h followed by quenching in water showing a region near the ferrite–austenite interface. Back scattered electrons. A indicates austenite, N indicates chromium nitride and S indicates sigma phase. Etching: V2A-Beize.

**Table 3.** Chemical composition of sigma phase and austenite (wt%), products of ferrite decomposition, in the sample aged at 860°C for 10 h.

| Element | Sigma Phase | Austenite |
|---|---|---|
| Fe | 51.8 | 62.8 |
| Cr | 29.6 | 19.3 |
| Si | 1.7 | 0.9 |
| Mn | 16.9 | 17.0 |

**Table 4.** Vickers microhardness of parent ferrite after aging heat treatments at 860°C.

| Aging time (min) | Vickers Microhardness (0.2 kg) |
|---|---|
| 15 | 913 ± 80 |
| 60 | 859 ± 228 |
| 600 | 820 ± 119 |

Chemical composition measurements showed higher levels of chromium and silicon in the sigma phase areas than in the austenite areas. The sigma phase identification was straightforward because this phase occurrence is favoured in ferrite and in ferrite–austenite interfaces. Austenite was easily identified due to its chemical composition analysis, which showed the lowest level of chromium.

**Table 4** shows the results of Vickers microhardness of the samples aged at 860°C for 15, 60 and 600 min and quenched in water. Aging for only 15 min was enough to cause a microhardness increase of about 600 HV.

3.2.2. Phase Transformations in Austenite

Austenitic regions, *e.g.* austenitic grains in the microstructure of the duplex steel, had about 1.0 wt% of nitrogen in solid solution,[10] in the solution annealed condition. Aging heat treatments caused chromium nitride precipitation, as shown in Fig. 5. These nitrides were identified as $Cr_2N$[12] using X-ray diffraction (Fig. 3). Nitride precipitation displayed a typical morphology and it looks like carbon steel pearlite. This morphology is a result of discontin-

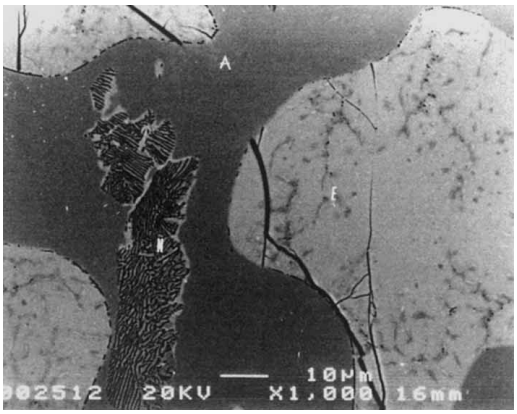


**Fig. 6.** Scanning electron microscopy micrograph of the sample aged at 860°C for 1 h indicates that parent ferrite phase transformed into sigma phase and austenite. Back scattered electrons. A indicates austenite, N indicates chromium nitride and F indicates the parent ferrite. Etching: V2A-Beize.

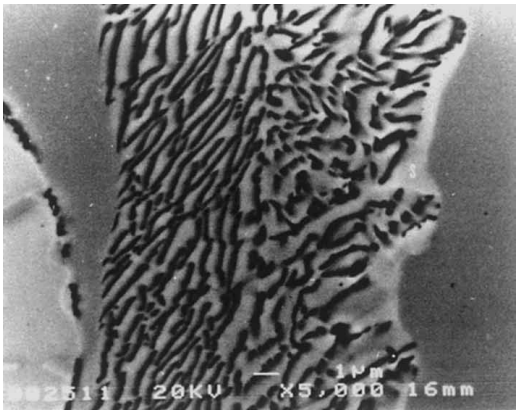


**Fig. 7.** Scanning electron microscopy micrograph of the sample aged at 860°C for 1 h. Back scattered electrons. S indicates sigma phase. Etching: V2A-Beize.

uous precipitation and is called "false pearlite".[13] X-ray diffraction analysis combined with observations using optical and scanning electron microscopy made the identification of chromium nitride possible as well as the precipitation mode. Some chromium nitrides seem to precipitate at ferrite-austenite interfaces as shown in the Fig. 5. This behaviour is more characteristic of the samples aged at low temperatures for longer periods of time. Sigma phase formation was observed in austenite as well, and it occurred near the chromium nitride discontinuously precipitated colonies.

**Figures 6** and **7** show the morphology of chromium nitrides and sigma phase formation. Figure 6 also shows cracks in the regions of transformed parent ferrite.

**Table 5** shows results of austenite lattice parameter measurements obtained by using X-ray diffraction after solution annealing and after some aging heat treatments. These results show a decrease in the lattice parameter of austenite during the aging heat treatments. The decrease of the austenite lattice parameter was caused by the nitrogen impoverishment of the solid solution due to chromium nitride precipitation. **Table 6** shows Vickers microhardness measurements of parent austenite after chromium nitride precipitation and sigma phase formation. Vickers microhardness measurements give an additional evidence of sigma

**Table 5.** Lattice parameters of austenite after solution annealing and after aging heat treatments at 860°C.

| Sample | Lattice parameter (Å) |
|---|---|
| Solution annealed | 3.637 |
| Aged for 15 min | 3.630 |
| Aged for 60 min | 3.624 |
| Aged for 600 min | 3.597 |

**Table 6.** Vickers microhardness of parent austenite (A) after the aging heat treatments at 860°C.

| Aging time (min) | Vickers Microhardness (0.2 kg) |
|---|---|
| 15 | 341 ± 57 |
| 60 | 353 ± 69 |
| 600 | 820 ± 119 |

**Table 7.** Chemical composition of sigma phase in austenite (wt%) in the sample aged at 860°C for 10 h followed by quenching in water.

| Element | Sigma Phase |
|---|---|
| Fe | 60.6 |
| Cr | 22.4 |
| Si | 1.1 |
| Mn | 15.9 |

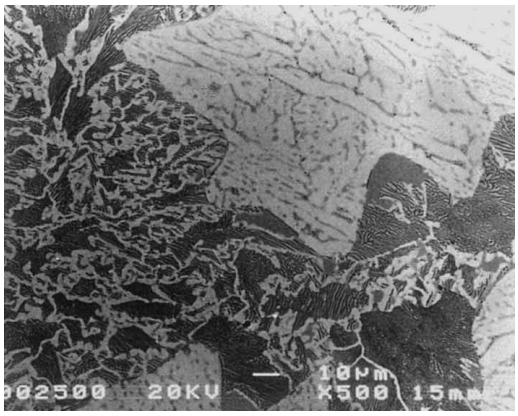


**Fig. 8.** Scanning electron microscopy micrograph of the sample aged at 860°C for 10 h followed by quenching in water. Dark regions show chromium nitride precipitation, light regions show sigma phase precipitation. Back scattered electrons. Etching: V2A-Beize.

phase formation in austenite. Sigma phase, like chromium nitride, is very hard.

**Table 7** displays the chemical composition of sigma in parent austenite. Sigma phase formed in austenite shows lower levels of chromium than that formed in ferrite.

**Figure 8** shows precipitation in the parent ferrite and in the parent austenite. In Fig. 8 it can be observed austenite transformation close to completion into chromium nitrides and sigma phase.

3.2.3. Time–Temperature–Transformation (TTT) Diagrams

The results of this work made it possible to drawn the TTT diagrams shown in **Fig. 9**. The comparison between the precipitation kinetics results of this paper (Fe–Cr–Mn system) to the kinetics results of the Fe–Cr–Ni systems[2,3] shows that Fe–Cr–Mn has slower precipitation reactions.

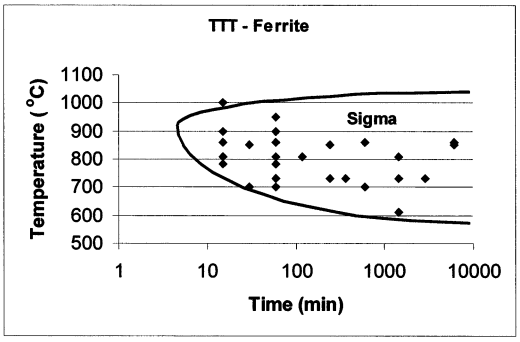


a)

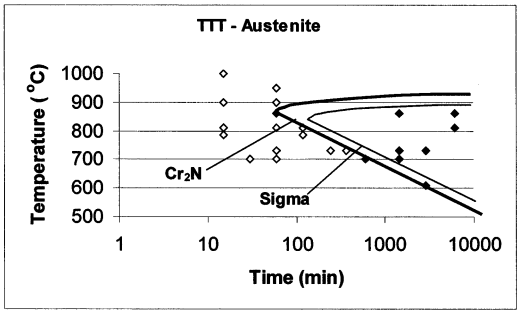


b)

**Fig. 9.** TTT diagrams of the 25%Cr–16%Mn–0.54%N duplex ferritic–austenitic stainless steel in ferrite (a) and in austenite (b).

## 4. Discussion

In the literature,[4,6,14] it can be frequently found precipitation studies in steels with similar composition, although their levels of chromium were always lower than that of the steel used in present work. Besides that, those works deal with austenitic steels instead of duplex steel. The nitrogen content of the 25%Cr–17%Mn steel used in this work was not enough to completely stabilize the austenite phase. High levels of chromium and the weak austenitizing effect of manganese, which is lower than that of nickel, led to a duplex microstructure of 25%Cr–17%Mn–0.54%N steel in instead of an austenitic one.

The ferrite phase of the present steel is very unstable at aging temperatures between 600 and 1 000°C. The results showed that aging heat treatments of only 15 min were enough to produce ferrite decomposition. The replacement of parent ferrite by sigma phase and austenite shows that ferrite decomposition in the studied steel occurred by the eutectoid reaction: ferrite⇒sigma phase+austenite ($\alpha = \sigma + \gamma$).

It was also observed the occurrence of cracks in the samples after some aging heat treatments. Sigma phase is fragile and the cracks probably occurred during quenching.

The austenite of the duplex stainless steel had a very high nitrogen content; about 1.0 wt%. This high nitrogen supersaturation favoured the discontinuous mode of chromium nitrides precipitation.[2,3] Discontinuous precipitation of chromium nitrides was observed in steels with similar composition,[4,6,14] however with a fully austenitic microstructure. There were some peculiarities in discontinuous precipitation occurrence in the steel used in the present study: i) the occurrence of discontinuous precipitation of nitrides in a duplex stainless steel was observed for the first time; ii) the discontinuously precipitated colonies were predominantly found inside the grains; iii) it was not observed continuous precipitation of nitrides inside the grains such as in another austenitic steels with high nitrogen content.[2,3]

Sigma phase formation occurred in austenite near discontinuously precipitated chromium nitride colonies. Besides that, sigma does not dissolve nitrogen and its precipitation should occur in the nitrogen-impoverished regions. Sigma phase in austenite must be an evidence of the nitrogen gradient formation near the reaction front during discontinuous precipitation. A possible reason for the existence of a nitrogen gradient is the great difference between the diffusion coefficient of nitrogen and the diffusion coefficient of chromium in the matrix. The reaction that describes sigma phase formation in austenite probably is one of the two reactions: 1. austenite impoverished in nitrogen⇒ferrite ($\gamma_{\downarrow N} \Rightarrow \alpha$) and then ferrite⇒sigma phase+austenite ($\alpha \Rightarrow \sigma + \gamma$) or 2. austenite impoverished in nitrogen⇒sigma phase ($\gamma_{\downarrow N} \Rightarrow \sigma$).

## 5. Conclusions

The experiments performed in this work, the analysis and discussion of the results lead to the following conclusions.

(1) Nitrogen addition of 0.54 wt% to the 25%Cr–17%Mn steel was not enough to form a fully austenitic microstructure; consequently a ferritic–austenitic duplex microstructure was formed.

(2) The ferritic phase of the duplex microstructure decomposes very fast into sigma phase and austenite by the eutectoid reaction: ferrite⇒sigma phase+austenite. ($\alpha = \sigma + \gamma$).

(3) The phase that first precipitates in the austenite of the duplex microstructure was the chromium nitride. This phase occurred with a peculiar morphology, similar to pearlite in carbon steels.

(4) Sigma phase was also formed in the austenitic phase after chromium nitride precipitation and it occurred near the nitrides colonies.

(5) The reaction that describes sigma phase formation in austenite indicates that one of the two possibilities can occur: 1. austenite impoverished in nitrogen⇒ferrite ($\gamma_{\downarrow N} \Rightarrow \alpha$) and then ferrite⇒sigma phase+austenite ($\alpha \Rightarrow \alpha + \gamma$) or 2. austenite impoverished in nitrogen⇒sigma phase ($\gamma_{\downarrow N} \Rightarrow \sigma$).

(6) Chromium nitrides precipitation in austenite was slower in the Fe–Cr–Mn–N system (present work) than in the Fe–Cr–Ni–N system (literature).

**Acknowledgments**

The authors are grateful to Prof. Dr. J. D. T. Capocchi (University of São Paulo, Brazil) and to Dr. F. Siciliano, Jr. (McGill University, Montreal, Canada) for going through the manuscript meticulously. The authors would like to acknowledge the support of the Conselho Nacional de Desenvolvimento Científico e Tecnológico (CNPq, Brazil).

REFERENCES

1) P. Reed: *JOM*, **41** (1989), 16.

2) I. F. Machado and A. F. Padilha: *Steel Res*., **67** (1996), 285.
3) I. F. Machado, A. M. Kliauga and A. F. Padilha: *Steel Res*., **69** (1998), 381.
4) R. Presser and J. M. Silcock: *Met. Sci.*, **17** (1983), 241.
5) W. Reick, M. Pohl and A. F. Padilha: *ISIJ Int.*, **38** (1998), 567.
6) F. Vanderschaeve, R. Taillard and J. Foct: *J. Mater. Sci.*, **30** (1995), 6035.
7) W. Reick: Dr.-Ing. Thesis, Ruhr-University, Bochum, Germany, (1993).
8) L. A. Norstrom, S. Petersson and S. Nordin: Z. *Werkstofftech.*, **12** (1981), 229.
9) G. Petzow: Metallographisches Ätzen, Gebrüder Bornträger, Berlin, (1984).
10) M. Pohl, F. Wischnowski and A. Ibach: Fortschritte in der Metallographie (Progress in Metallography)., ed. by M. Kurz and M. Pohl, Germany, DGM Informationsgesellschaft Verlag, Oberursel, (1995), 363.
11) Powder Diffraction File Nr. 5-0708 ($\sigma$-FeCr), Joint Committee on Powder Diffraction Standards.
12) Powder Diffraction File Nr. 35-803 ($\beta$-$Cr_2N$), Joint Committee on Powder Diffraction Standards.
13) J. Menzel; W. Kirschner; G. Stein: *ISIJ Int.*, **36** (1996), 893.
14) N. C. Santhi Srinivas and V. V. Kutumbarao: *Scripta Mater.*, **37** (1997), 285.